Revised

Linker dependent dimensionality in Zn(II)-coordination polymers containing a flexible bis-pyridyl-bis-amide ligand

Davide Balestri,[a] Davide Costa,[a] Alessia Bacchi,[a] Lucia Carlucci,[b] Paolo Pelagatti[a]*

[a]Department of Chemical Sciences, Life Sciences and Environmental Sustainability, University of Parma, Parco Area delle Scienze 17/A, 43124 Parma, Italy.

[b]Department of Chemistry, Università degli Studi di Milano, via Golgi 19, 20133 Milano, Italy.

Corresponding Author: Paolo Pelagatti, paolo.pelagatti@unipr.it

Abstract

A bis-pyridyl-bis-amide ligand containing a biphenylene scaffold was combined with four different dicarboxylic acids in the presence of $Zn(NO_3)_2 \cdot 6H_2O$ under solvothermal conditions, using DMF as solvent. The corresponding coordination frameworks were structurally characterized by single crystal diffraction analysis, the topological and thermal analysis were also conducted. The removing of the included DMF was investigated through solvent assisted activation protocol, the final outcomes being determined by ^{1}HNMR analysis. The dimensionality of the solid networks depends on the type of dicarboxylic acid employed. The use of isophthalic acid and 5-amino-isophthalic acid led to the isolation of 2D-frameworks (**PUM20** and **PUM32**, of topological type **3,5L2**) , while a 1-D polymer was obtained using 2-methoxy-isophthalic acid (**PUM30**, of topological type SP 1-periodic). Finally, the use of terephthalic acid led to a pillared 3D-structure (**PUM198**, of topological type **fet**).

Keywords

Coordination Polymers - Pillared MOFs – Amide linker – Zinc(II) – Topology

1. Introduction

The synthesis of Mixed-Ligand Coordination Polymers (MLCPs), also called heteroleptic CPs, relates to the construction of crystalline frameworks containing two different ligands combined with metal nodes. Hence, the self-assembly process occurring under solvothermal conditions is certainly more complicated than the one involving the construction of homoleptic CPs. However, MLCPs allow to reach more sophisticated structures with higher degree of functionalization, which in turn leads to tailoring of the material function.[1][2][3] The design usually followed for the construction of MLCPs is based on the so-called pillaring-strategy.[4][5] One of the most common methods to get pillaring passes through the construction of the paddlewheel-like SBU $M_2(O_2CR)_4L_2$.[6] Use of dicarboxylate linkers leads to formation of 2D planes containing the dinuclear SBUs connected by the dicarboxylate dianions. The planes can then be linked by divergent ligands L occupying the axial positions of the paddlewheel units, creating a 3D pillared framework. In this case, the term mixed-ligand Metal-Organic-Frameworks (MLMOFs) should be used, to emphasize the 3D dimensionality of the polymer. As pillaring struts, bis-pyridines are very common, the length of which dictates the dimension of the resulting channels, and then the porosity of the final material.[7] Following this approach, we chose to combine four different dicarboxylic acids, namely isophthalic acid H_2ipa, 2-methoxy-isophthalic acid H_2(MeO)-ipa, 5-

Revised

aminoisophthalic acid $H_2(NH_2)$-ipa and terephthalic acid H_2tpa, with the bis-pyridine-bis amide ligand **L1** reported in Scheme 1.
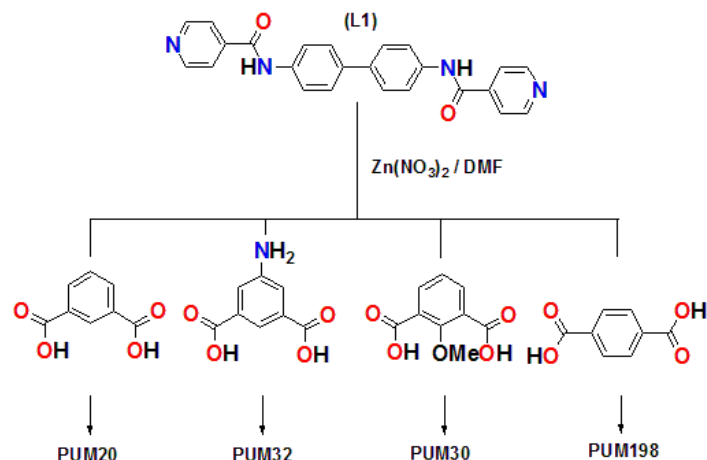
Scheme 1 General scheme of the synthesis of the MOFs discussed in this paper

Our aim was to evaluate the effect the linear or bent geometry of the selected dicarboxylic acids has on the possibility of reaching the pillared architecture. As depicted in Scheme 1, under solvothermal conditions four new polymeric materials were isolated, namely $\{[Zn_2(\textbf{L1})_2(ipa)_2](4DMF)\}_n$ (**PUM20**), $\{[Zn(\textbf{L1})_{0.5}(MeO\text{-}ipa)(DMF)]\}_n$ (**PUM30**), $\{[Zn(\textbf{L1})(NH_2\text{-}ipa)](1.5DMF)\}_n$ (**PUM32**) and $\{[Zn_2(\textbf{L1})_2(tpa)_2](5DMF)\}_n$ (**PUM198**). PUM stands for Parma University Materials. Single crystal X-ray diffraction analysis conducted on all the compounds revealed the different dimensionality featuring the four polymeric materials, as well as the impact the different dicarboxylic linkers functionalization has on the hydrogen bond networks found in the crystalline frameworks. The topological description of the networks, their thermal behavior and the easiness of DMF removal/exchange were also investigated.

2. Experimental

2.1. Materials and physical measurements

All reagents and solvents were commercially available and used as received. The bis-pyridyl ligand **L1** was synthesized as previously reported.[8] ^{1}H-NMR were recorded on a 400 and 300 MHz Bruker instruments after dissolution of the materials in one drop of CF_3COOD and dilution with $(CD_3)_2SO$. Chemical shifts are reported in ppm relative to the solvent residual peak of deuterated DMSO (δH 2.50, δC 39.5). TGA analyses were performed on a Mattler Toledo TGA/DSC1 instrument (sample mass approximatively 5-10 mg) at a heating rate of $10°C\cdot min^{-1}$ in the temperature range 25-500 °C. The measurements were performed at atmospheric pressure under nitrogen (80 mL·min^{-1}). Elemental analyses were conducted by means of a FlashEA 1112 Series CHNS-O

Revised

2.2. Synthesis

Syntheses of the coordination networks were conducted under solvothermal conditions dissolving free ligands and $Zn(NO_3)_2 \cdot 6H_2O$ in DMF at room temperature in a 17 mL screw-capped Pyrex-glass tubes. The mixture was sonicated until complete dissolution of the reagents, then the sealed tube was immersed in a silicon oil bath, or in a pre-heated oven, thermostated at the desired temperature, for the time necessary to grow X-ray quality single crystals. Then the tube was slowly cooled at room temperature, the crystals were filtered off, washed with DMF and vacuum dried. The phase purity of the isolated compounds was checked by XRPD analysis by comparison with the diffractograms calculated from X-ray single crystal structures.

*2.2.1. Synthesis of **PUM20** $\{[Zn_2(\textbf{L1})_2(\textbf{ipa})_2](4DMF)\}_n$*

H_2ipa (16.6 mg, 0.1 mmol), **L1** (19.7 mg, 0.05 mmol) and $Zn(NO_3)_2 \cdot 6H_2O$ (29.7 mg, 0.1 mmol) in 10 mL of DMF. The solution was heated at 80 °C for two days. Yellow plate crystals were collected. Yield: 60% based on Zn. Anal. Calcd. for $C_{76}H_{72}N_{12}O_{16}Zn_2$ (found): C, 59.70 (60.01); H, 4.75 (4.72); N, 10.99 (11.02).

*2.2.2. Synthesis of **PUM30** $\{[Zn(\textbf{L1})_{0.5}(\textbf{MeO-ipa})(DMF)]\}_n$*

$H_2(MeO)$-ipa (19.62 mg, 0.1 mmol), **L1** (19.7 mg, 0.05 mmol), $Zn(NO_3)_2 \cdot 6H_2O$ (29.7 mg, 0.1 mmol) in 10 mL of DMF. The solution was heated at 80 °C. After 10 days the solution was still clear. After slow cooling at room temperature, large crystals were collected. Yield: 58% based on Zn. Anal. Calcd. for $C_{30}H_{36}N_5O_9Zn$ (found): C, 53.60 (53.66); H, 5.40 (5.34); N, 10.42 (10.38).

*2.2.3. Synthesis of **PUM32** $\{[Zn(\textbf{L1})(\textbf{NH}_2\textbf{-ipa})](1.5DMF)\}_n$*

$H_2(NH_2)$-ipa (18.115 mg, 0.1 mmol), **L1** (19.7 mg, 0.05 mmol) and $Zn(NO_3)_2 \cdot 6H_2O$ (29.7 mg, 0.1 mmol) in 10 mL of DMF. The solution was heated at 110 °C for two days. Yellow plate crystals were collected. Yield: 65% based on Zn. Anal. Calcd. for $C_{36.5}H_{40.5}N_{7.5}O_{8.5}Zn$ (found): C, 64.31 (64.25); H, 5.99 (6.00); N, 15.41(15.38).

*2.2.4. Synthesis of **PUM198** $\{[Zn_2(\textbf{L1})_2(\textbf{tpa})_2](5DMF)\}_n$*

H_2tpa (66 mg, 0.44 mmol), **L1** (80 mg, 0.2 mmol) and $Zn(NO_3)_2 \cdot 6H_2O$ (120 mg, 0.4 mmol) in 41 mL of DMF. The solution was heated at 80°C for 4 days, then slowly cooled at room temperature. The yellow crystals were collected and washed with DMF. Yield: 71% based on Zn. Anal. Calcd. for $C_{77}H_{77}N_{13}O_{17}Zn_2$ (found): C, 58.26 (58.55); H, 4.89 (4.65); N, 11.47(11.38).

2.2.5 Crystallographic data

X-ray single crystal data collections were performed at Elettra Sincrotrone (Trieste, Italy) on beamline XRD1.[9] The beamline spectra (produced by a NdBFe multipole wiggler) was monochromatized to 17.71KeV (0.700Å) through a Si(111) double crystal monochromator and focused to obtain a beam size of 0.2×0.2 mm FWHM at the sample (photon flux 10^{12}-10^{13} ph·sec^{-1}). Crystals were taken from the mother liquor and dipped in NHV oil (Jena Bioscience GmbH) and mounted on the goniometer head with a nylon loop (0.05-0.3 mm). Complete datasets were collected at 100 K (nitrogen stream supplied through an Oxford Cryostream 700) through the rotating crystal method. For triclinic crystals complete datasets were obtained merging two different data

3

Revised

collections done on the same crystal, mounted with different orientations. Data were acquired using a monochromatic wavelength of 0.700 Å on a Pilatus 2M hybrid-pixel area detector. The diffraction data were indexed and integrated using XDS.[10] Scaling were done using CCP4-Aimless code.[11][12] The structures were solved by the dual space algorithm implemented in the SHELXT code[13] in Olex2.[14] Fourier analysis and refinement were performed by the full-matrix least-squares methods based on F2 implemented in SHELXL-2014.[15] For all the structures, anisotropic displacement parameters were refined except for hydrogen atoms. DMF molecules were located on the difference electron density maps, and mostly modelled with restrained geometry; in most cases DMF molecules appeared distributed over pairs of mutually exclusive disordered positions. We deliberately chose not to use the *squeeze* procedure for the final refinement, to obtain the best possible description of the structuring of guest DMF molecules in the materials, and this resulted in some cases to quite high residual peaks, which were related to further unaccounted disorder concerning the modelling of DMF molecules. Large residual electron density. **PUM198** shows signs of twinning evidenced by high residuals of ghosts distributed around the skeleton of the MOF structure. ~~CCDC: 1846378-184681 contain the supplementary crystallographic data for the reported compounds. These data can be obtained free of charge from The Cambridge Crystallographic Data Centre via https://www.ccdc.cam.ac.uk/structures.~~ Table 1 reports crystal data and refinement details.

Table 1.

Crystallographic data and structural refinement

|	PUM20	PUM32	PUM30	PUM198
Empirical formula	$C_{64}H_{44}N_8O_{12}Zn_2$, $3.5(C_3H_7NO)$	$C_{32}H_{23}N_5O_6Zn$, $2(C_3H_7NO)$	$C_{24}H_{22}N_3O_7Zn$, $1.5(C_3H_7NO)$	$C_{64}H_{44}N_8O_{12}Zn_2$, $5(C_3H_7NO)$
Formula weight	1503.64	785.11	639.46	1598.52
Crystal system	triclinic	triclinic	triclinic	monoclinic
Space group	P-1	P-1	P-1	P21/c
a(Å)	9.956(2)	9.6895(19)	7.9058(16)	24.3401(4)
b(Å)	17.427(4)	10.051(2)	9.2028(18)	17.3778(3)
c(Å)	20.581(4)	19.887(4)	21.316(4)	17.8506(2)
α(°)	99.92(3)	79.05(3)	97.86(3)	90
β(°)	103.95(3)	76.39(3)	95.75(3)	94.4920(10)
γ(°)	92.17(3)	77.39(3)	105.84(3)	90
Volume(Å^3)	3402.1(13)	1817.3(7)	1462.5(6)	7527.2(2)
Z	2	2	2	4
ρcalc (g/cm^3)	1.468	1.435	1.452	1.411
F(000)	1560.0	816.0	666.0	3329.0
Crystal size/mm^3	$0.20 \times 0.13 \times 0.11$	$0.2 \times 0.13 \times 0.11$	$0.15 \times 0.10 \times 0.09$	$0.15 \times 0.11 \times 0.10$
2Θ range for data collection/°	2.044 to 55.636	2.098 to 58.17	1.92 to 51.884	3.226 to 55.636
Index ranges	-13 ≤ h ≤ 12, -23 ≤ k ≤ 22, 0 ≤ l ≤ 27	-12 ≤ h ≤ 13, -13 ≤ k ≤ 13, 0 ≤ l ≤ 27	-9 ≤ h ≤ 9, -11 ≤ k ≤ 11, 0 ≤ l ≤ 26	-32 ≤ h ≤ 32, -23 ≤ k ≤ 23, -23 ≤ l ≤ 23
Reflections collected	94512	64143	18511	114846
Independent reflections	16680 [Rint = 0.0345, Rsigma = 0.0329]	10061 [Rint = 0.0380, Rsigma = 0.0220]	5852 [Rint = 0.0861, Rsigma = 0.0781]	18575 [Rint = 0.0741, Rsigma = 0.0395]
Data/restraints/parameters	16680/488/897	10061/182/522	5852/733/509	18575/839/994

Revised

Goodness-of-fit on F2	1.042	1.099	1.119	1.035
Final R indexes [I>=2σ (I)]	R1 = 0.0658, wR2 = 0.1738	R1 = 0.0557, wR2 = 0.1474	R1 = 0.1001, wR2 = 0.2720	R1 = 0.1110, wR2 = 0.3048
Largest diff. peak/hole (eÅ^{-3})	3.99/-1.80	1.46/-1.68	2.24/-1.61	1.73/-1.22

3. Results and Discussion

3.1. *PUM20*

The asymmetric unit of **PUM20** contains two Zn^{2+} ions, two **L1** ligands and two fully deprotonated isophthalate ipa^{2-} anions. The exclusive SBU found in the framework has formula [$Zn_2(\mu\text{-COO})_2(\kappa^1\text{-COO})_2(py)_2$] (Figure 1a-b).
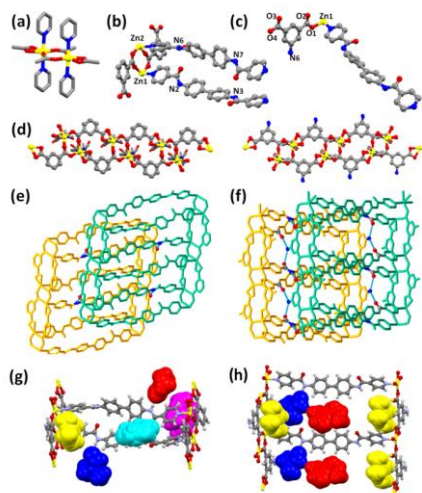

Fig. 1 (a) SBU unit for **PUM20** and **PUM32** (b) Asymmetric unit of **PUM20** (c) Asymmetric unit of **PUM32** (d) 1D-ribbonlike chains for **PUM20** (left) and **PUM32** (right) (e) Schematic view of hydrogen bond N–H···O contacts between adjacent 2D-layers for **PUM20** (f) Schematic view of hydrogen bond NH$_2$···O=C and N–H···O interactions involving 2D-layers for **PUM30** (g) localization of five independent DMF molecules in **PUM20**, with two of them (red and blue) hydrogen bonded to the amide, the other three disordered (h) localization of three independent DMF molecules in **PUM32**, with one of them (blue) hydrogen bonded to the amide, the other two, red and yellow, disordered.

Each Zn lies in a distorted octahedral environment, defined by two nitrogens of two mutually trans **L1** ligands, and three different COO$^-$ groups belonging to three different ipa^{2-} ions. The coordinating behavior of the two carboxylates of each ipa^{2-} ion is different. One is bridging the two Zn^{2+} ions, while the other is κ^2-chelating. The Zn-N$_{(py)}$ and Zn-O$_{(carboxylate)}$ distances agree with those found in other analogous coordination environments. A search in the CCDC database showed that this SBU is rarely found in MOFs, being found only in a couple of

5

Revised

Co^{2+} and Ni^{2+} containing materials.[16] The Zn^{2+} ions are bridged by ipa^{2-} ions forming 1D-ribbonlike chains running along the *a* axis, containing an alternate arrangement of 8- and 16-membered rings, as depicted in Figure 1d (left). Two carboxylic groups bridge two Zn^{2+} to form an eight-membered ring, while two chelating carboxylic groups of two ipa^{2-} bridge two Zn^{2+} to form a 16-membered ring. Within the eight and sixteen membered rings the Zn-Zn distances are 4.25Å and 7.14Å, respectively. The resulting chains are interlinked by the **L1** ligands forming a 2D layer, as depicted in Figure 2a.
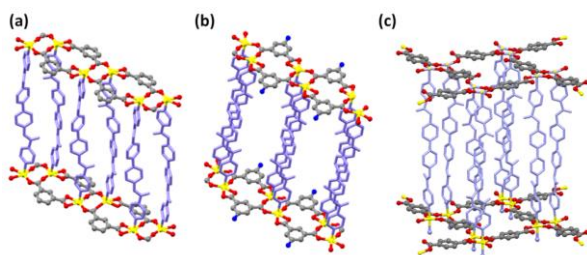
Fig. 2. Pillaring of ribbons (**PUM20** = a, **PUM32** = b) and 2D grids (**PUM198** = c) by ligand **L1**. Flexibility of **L1**, manifested by different torsional conformations, is related to hydrogen bond interactions with DMF (not shown) and neighboring networks.

The two rings of the biphenyl scaffold are twisted with similar dihedral angles of -26° and -36° on the two independent **L1** moieties. The carbonyl groups of the amide functions on the two **L1** ligands display a staggered conformation, forming O=C…C=O dihedral angles of -92° and 120° respectively. In fact, the two amide groups on each ligand play different supramolecular roles in the crystal assembly. Namely, the 2D-layers are held together by hydrogen-bonds connecting one of the two N-H amide function of each of the two independent molecules of **L1** belonging to a layer with an oxygen of a chelating carboxylate group belonging to opposite adjacent layers, as depicted in Figure 1e. The other NH amide on each ligand is used to interact with the solvent filling the space between the layers. The layered structure in fact hosts DMF molecules with different supramolecular arrangements: two of them are firmly linked to the framework by the above described N-H···O hydrogen bonds (Figure 1g). Other three DMF molecules have been located fitting inside cavities centered on inversion centers of the structure; these are loosely bound by the framework, being disordered over multiple positions, and likely to be more labile than the hydrogen bonded ones. The thermal stability of **PUM20** is respectably high if considered the supramolecular packing of the framework. Thermal decomposition occurs at 388°C which is preceded by a multi-step desolvation between 60 and 271°C, mirroring the different stability of the DMF solvation molecules, and corresponding to an overall weight loss percentage of 18.4%. This relates to 4 molecules of DMF, as anticipated by elemental analysis. Figure S1a shows the volume potentially accessible to solvent in **PUM20**. The complete formula of **PUM20** is then [Zn$_2$(**L1**)$_2$(**ipa**)$_2$]·4DMF.

3.2 PUM32

The asymmetric unit of **PUM32** contains a Zn^{2+} ion, one ligand **L1** and one **NH$_2$-ipa^{2-}** anion (Figure 1c). The framework contains only one type of SBU, which is equivalent to the one found in **PUM20**. Also, the coordination environment of the metal is the same of that seen in **PUM20**, with bond distances ranging in the expected intervals. Similarly to **PUM20**, the **NH$_2$-ipa^{2-}** anions bridge the Zn^{2+} cations forming 1D-ribbon like chains (Figure 1d), with the distances between the Zn^{2+} ions in the 8- and 16-membered rings of 4.1 and 7.5Å,

**Commentato [P1]:** La frase spiega già quanto richiesto dal reviewer 2 sulla tga

respectively. The ribbons are linked in layers by the **L1** ligands, similarly to **PUM20** (Figure 2b). The main structural difference between the layers of **PUM20** and **PUM32** is represented by the conformation of the amidic C=O groups in the pillar **L1** ligands, that in **PUM32** adopt a *cisoid* configuration (O=C…C=O torsion is 19°), related to the role that amidic groups have in the assembly of the layers. The NH_2 groups on the **NH_2-ipa^{2-}** anion are in fact engaged in hydrogen bonds with one amide C=O group of **L1** belonging to the same adjacent net, with which the second amide makes the same amide NH…carboxylate hydrogen bonds found in **PUM20** (Figure 1f). The cell content is completed by one ordered DMF molecule hydrogen bonded to the NH of the amide group involved in the interaction with the **NH_2-ipa^{2-}** amine, and two DMF partially disordered around inversion centers, similarly to **PUM20** (Figure 1h). Thermal behavior shows again a high stability of the supramolecular network which decomposes at about 370°C. Decomposition is preceded by a featureless multi-step desolvation in the range 70-360°C, with a loss weight percentage of 16%. This corresponds to 1.5 molecules of DMF, in good agreement with the elemental analysis. Figure S1b shows the volume potentially accessible to solvent in **PUM32**. The whole formula of **PUM32** is then [Zn(**L1**)(**NH_2-ipa**)]·(1.5DMF).

3.3 PUM30

The asymmetric unit of **PUM30** contains one Zn^{2+}, one **MeO-ipa^{2-}** anion, half molecule of **L1** and a coordinated DMF molecule (Figure 3a), disordered on two positions. The SBU has formula [Zn(κ^2-COO)(κ^1-COO)(py)(DMF)], the metal having a square pyramidal coordination geometry, satisfied by a chelating COO group of a **MeO-ipa^{2-}** ion, one monodentate COO group of a second **MeO-ipa^{2-}** anion, one pyridine and one DMF molecule. The bridging dicarboxylate anions line the Zn atoms along the *b* direction, while ligand **L1** bridges two antiparallel alignments of metal ions, forming the ladder motif depicted in Figure 3b. The amidic C=O groups of **L1** adopt a *transoid* configuration (O=C…C=O torsion angle=165°), being distributed on two disordered orientations around the center of inversion to avoid the phenyl to be coplanar.
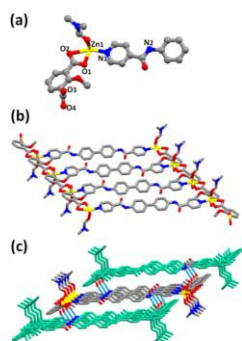
Fig. 3 (a) Asymmetric unit of **PUM30** (disorder of DMF not shown for clarity) (b) Stick view of the 1D framework structure in **PUM30**. (c) Schematic view of the 3D supramolecular framework formed by N–H···O hydrogen bond interactions.

Revised

The ladders are held together by hydrogen bonds between the N-H groups of **L1** and the dangling carboxylic C=O group not involved in coordination (Figure 3c). **PUM30** can then be classified as a 1D coordination polymer. The thermogravimetric analysis shows 19% weight loss in the temperature range from 100°C to 358°C, with decomposition occurring at about 360°C. The weight loss preceding decomposition is attributed to the departure of two molecules of DMF, one corresponding to that coordinated to Zn and another included over two disordered sites in the framework (Figure S2), in good agreement with the elemental analysis. Figure S1c shows the volume potentially accessible to solvent in **PUM30**. The whole formula of **PUM30** is then [Zn(**L1**)$_{0.5}$(**MeO-ipa**)(DMF)](DMF).

3.4 PUM198

The asymmetric unit of **PUM198** contains two Zn^{2+} ions, two terephthalate anions, two **L1** ligands and five molecules of DMF, of which three are disordered. The SBU is formed by Zn nodes of the type [Zn$_2$(κ^1-COO)$_2$(κ^2-COO)$_2$(**L1**)$_4$] (Figure 4a). The two carboxylic functions behave differently: one COO group bridges two metal ions belonging to the aforementioned SBU, while the other COO group is monodentate to another Zn^{2+} ion belonging to another SBU (Figure 4b). The Zn···O and Zn···N bond distances fall in the expected ranges. The overall structural motif is doubly interpenetrated pillared framework (Figure 4c), where the carboxylate groups and the Zn^{2+} ions define 2D planes, which are then pillared by ligand **L1**, as depicted in Figure 2c. The C=O group not involved in coordination forms a C=O···H-N hydrogen bond with a neighboring **L1**. Channels of 5.6×17.4Å dimension run along the *c* axis direction (Figure S1d), and are filled by DMF molecules, as depicted in Figure 4d. After removal of solvent electron density, the calculated void volume corresponds to 28% of unit cell, equal to 2125Å^3 (Contact Surface Function by Mercury). The thermogravimetric trace indicates a good thermal stability, with decomposition occurring at around 400°C. This is preceded by solvent extrusion from room temperature to 250°C, with a weight loss of 19%. This would correspond to 4 molecules of DMF, consistent with the 5 partially disordered solvation sites found by X-ray structure determination and with elemental analysis data. A partial desolvation of the most mobile DMF in the pores prior to TGA experiment could explain the lower amount of extruded solvent detected by thermal analysis. The whole formula of **PUM198** is then [Zn$_2$(**L1**)$_2$(**tpa**)$_2$]·(5DMF).

4. Topological analysis

In order to better elucidate the role of the four different dicarboxylic ligands and the action of hydrogen bonds on the self-assembly of **PUM20**-**30**-**32**-**198** we performed a detailed topological analysis by using the program ToposPro.[17] The topology of coordination networks, as well as that of the hydrogen bonded supramolecular arrays is analysed sequentially for all compounds. Compounds **PUM20** and **PUM32** are similar showing analogous coordination 2D motifs that, by simplification in both cases, lead to a 3,5-c network of topological type **3,5L2**, point symbol (4^2.6^7.8)(4^2.6) (Figure 5a). In this simplification the Zn^{2+} ions and ipa^{2-} or NH$_2$-ipa^{2-} ions behave, respectively, as the 5- and 3-c nodes. Such topological type is quite common within coordination networks and many examples, more than 500, are reported in ToposPro databases (inorganic.ttd). Different torsion angles for **L1** and the presence of a NH$_2$- group on the carboxylate ligand in **PUM32**, produce different hydrogen bond patterns in the two compounds (Figure 5b, c) and, consequently, the derived supramolecular arrays show diverse network topologies. In **PUM20** a 3D supramolecular array originates from the hydrogen bonds between one amidic N-H group of all **L1** and oxygen atoms of chelate carboxylate fragments belonging to adjacent parallel layers. Simplification of such 3D network, performed taking into account the hydrogen bond connections and selecting the Zn^{2+} ions as nodes, give a 3-nodal 3,4,5-c net of topological type **3,4,5T94**, point symbol (4^2.6^3.8)(4^2.6^5.8^3)(6^2.8) (Figure 5d).

8
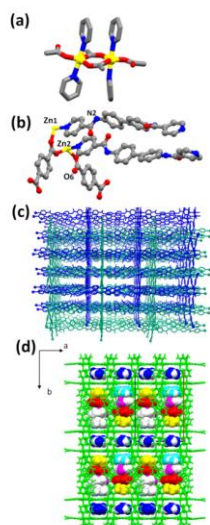
Fig. 4 a) SBU and asymmetric unit (b) for **PUM198**; c) interpenetrated pillared structure of **PUM198**, pores of 5.6×17.4Å dimension run along axis **c**; (d) five differently coloured independent DMF sites in the pores of **PUM198**.

In this resulting **3,4,5T94** net Zn^{2+} ions, isophtalate and **L1** ligands act as the 5-c, 4-c and 3-c nodes, respectively (Figure 5b). About 10 known examples of structures with such topology is given in MOF.ttd database of ToposPro. As in the previous case, also in **PUM32** each coordination layer is hydrogen bonded on both sides with adjacent layers to give a 3D supramolecular array. However, due to the presence and involvement of the amino groups in the hydrogen bond patterns (Figure 5c) the topology of the supramolecular network is different. Taking into account the hydrogen bonds and selecting the Zn^{2+} ions as nodes, the simplification process for **PUM32** results in a binodal 5,6-c 3D network of topological type **yav**, point symbol $(4^3.6^6.8)_2(4^6.6^9)$ (Figure 5e). The two 5-c nodes in this network are, respectively, the zinc atoms and the ligands **L1**, while the 6-c one lie on the NH_2-isophtalate fragment. About 30 examples of this topology are reported in ToposPro database (topos&RCSR.ttd).

Compound **PUM30** contains parallel 1D coordination motifs of the very common ladder-like type, classified as SP 1-periodic in ToposPro (Figure 6a). Adjacent parallel ladders interact each other through hydrogen bonds between the two N-H bonds of each **L1** and the uncoordinated oxygen atoms of the metoxy-isophthalate fragments giving a 2D supramolecular array (Figure 6a, c).

9
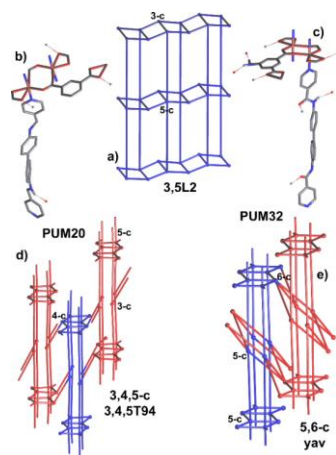
Fig. 5 a) Simplified view of the 2D coordination network for **PUM20** and **PUM32**; b) and c) hydrogen bond patterns for **PUM20** and **PUM32**, respectively; d) and e) views of the simplified 3D networks derived from the 3D supramolecular array for **PUM20** and **PUM32**, respectively.

Network simplification performed according to usual procedure, that is taking into account hydrogen bonds and selecting Zn^{2+} ions as nodes, results in a binodal 3,4-c 2D net of topological type **3,4L90**, point symbol $(6^2.8^4)(6^2.8)_4$ (Figure 6c). In the simplified **3,4L90** the 3-c nodes correspond to the Zn^{2+} ions and to the MeOipa^{2-} ions, and the 4-c ones lie in the middle of ligand **L1** (Figure 6c). More than 40 examples of such topology are reported in ToposPro database (1D_2D.ttd).
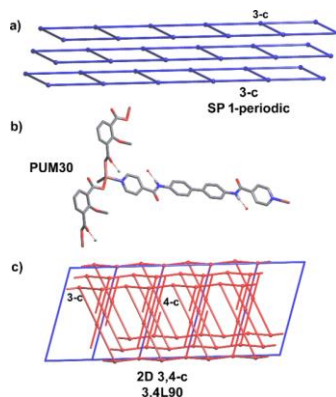
Fig. 6 a) Simplified view of the 1D coordination ladder for **PUM30**; b) hydrogen bond pattern for **PUM30**; c) view of a single simplified 2D networks (in red) derived from the supramolecular array for **PUM30**; in blue the superposition of a single ladder is highlighted.

Revised

Compound **PUM198**, as already described, show a pillared 3D coordination network 2-fold interpenetrated. Topological analysis, after simplification considering the Zn^{2+} ions as nodes, reveals that the 3D network is binodal 3,5-c of topological type **fet**, point symbol $(4.6^2)(4^6.6^6.8^3)$ (Figure 7a). In this network the 3- and 5-c nodes correspond to the barycenter of the terephthalate ligands and to the Zn^{2+} ions, respectively (Figure 7a). The two equivalent interpenetrating networks are related by a center of inversion and belong to class IIa.[18] The only hydrogen bond present in this structure involve one N-H bond of a single crystallographically independent **L1** ligand, and the uncoordinated oxygen atom of one terephthalate ligand. This C=O$\cdots$H-N interaction connect the two interpenetrated nets and if it is taken into account a complex self-penetrate 3D supramolecular array arises. The topological type **fet** is quite common within coordination networks and about 180 examples of single or interpenetrated structures are reported in ToposPro database (binodal.ttd).
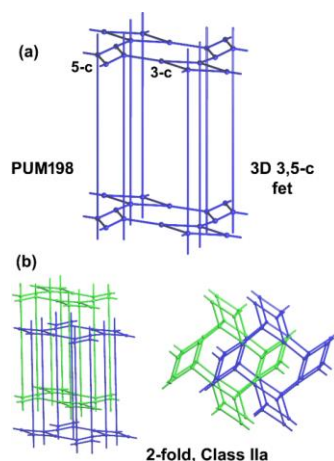
Fig. 7 a) Simplified view of a single 3,5-c 3D net of **fet** type for **PUM198**; b) two views of the 2-fold interpenetration for **PUM198**.

5. DMF exchange

Porosity is undoubtedly the main feature of CPs and MOFs and it is exploited mainly for hosting molecular species.[19][20] However, in order to host the guest molecules the pores must first be evacuated from the molecules of solvent trapped in their inside during the framework formation. This step is usually referred as activation.[21] This must be considered a delicate step, because evacuation of the framework can lead to collapse of the crystalline structure and closure of the pores, especially if conducted with the help of temperatures close to the high boiling point of the solvents usually employed for the syntheses, such as DMF. One of the activation protocol usually adopted because capable of maintaining intact the framework is the so-called solvent-assisted activation protocol (SAAP). This consists in replacing the molecules of DMF by repeated soakings of the native crystals in a low boiling solvent, which can then be subsequently removed by a gentle vacuum. Preliminary tests were conducted on **PUM20**, using cyclohexane and ethanol as exchanging solvents and monitoring the extent of

11

Revised

DMF exchange through ^{1}H NMR spectroscopy on crystals digested in a $CF_3COOD/(CD_3)_2SO$ mixture. The crystals were soaked for 48 hours at room temperature in the chosen solvent, and gently shacked by means of an orbital stirrer. The solvent was then refreshed and stirring was repeated for other 48 hours. ^{1}HNMR spectrum revealed that none of the DMF molecules had been replaced by cyclohexane, which neither was included in the crystals. The guest exchange was instead successful with ethanol, since the ^{1}H NMR spectrum revealed the complete absence of DMF and the inclusion of three molecule of ethanol (doublets at 3.42 ppm and triplet at 1.04 ppm, Figure S3). SAAP with ethanol was then successfully extended to **PUM32**. ^{1}H NMR spectrum revealed the complete removal of DMF with no inclusion of ethanol (Figure S4). In this case, however, desolvation of the framework led to loss of crystallinity, as evidenced by opacification of the crystals. In the case of **PUM198** SAAP was instead only partially successful. ^{1}H NMR spectroscopy indicated the removal of 4 out of the five molecules of DMF included in the native crystals, with no inclusion of alcohol (Figures S5-S6). As for **PUM32**, the SAAP led to opacification of the crystals. Remarkably, the situation did not change after exposure of the partially activated crystals to high vacuum (approximatively 10^{-6} torr), to indicate a strong binding of the molecules of DMF to the MOF walls.

Commentato [P4]: Questo risponde al reviewer 1 sulla porosità di pum198

6. Conclusions

Four mixed-ligand coordination polymers with different dimensionality obtained combining the bis-pyridyl-bis amide ligand **L1** with four different dicarboxylic ligands have been synthesized and structurally characterized. The linearity of terephthalic acid led to reach the targeted pillar structure which was found in **PUM198**, while V-shaped dicarboxylate anions, such as isophthalic acid and 5-amino-isophthalic acid, led to the isolation of 2D polymeric nets, whose three-dimensionality derive from supramolecular interactions, as found in **PUM20** and **PUM32**. In the case of 2-methoxy-isophthalic acid the network dimensionality is reduced to 1D, like in the case of **PUM30**.

Appendix A. Supplementary data

CCDC 1846378-184681 contain the supplementary crystallographic data for the reported compounds. These data can be obtained free of charge from The Cambridge Crystallographic Data Centre via https://www.ccdc.cam.ac.uk/conts/retrieving.html or from the Cambridge Crystallographic Data Centre, 12 Union Road, Cambridge CB2 1EZ, UK; fax: (+44) 1223-336-033; or e-mail: deposit@ccdc.cam.ac.uk.

References

[1] K.L. Mulfort, J.T. Hupp, Chemical reduction of metal-organic framework materials as a method to enhance gas uptake and binding, J. Am. Chem. Soc. 129 (2007) 9604–9605. doi:10.1021/ja0740364.

[2] A. Dhakshinamoorthy, A.M. Asiri, H. Garcia, Mixed-metal or mixed-linker metal organic frameworks as heterogeneous catalysts, Catal. Sci. Technol. 6 (2016) 5238–5261. doi:10.1039/C6CY00695G.

[3] D.M. Chen, N. Xu, X.H. Qiu, P. Cheng, Functionalization of metal-organic framework via mixed-ligand strategy for selective CO2sorption at ambient conditions, Cryst. Growth Des. 15 (2015) 961–965.

doi:10.1021/cg501758a.

[4]   Z. Chang, D.S. Zhang, Q. Chen, R.F. Li, T.L. Hu, X.H. Bu, Rational construction of 3D pillared metal-organic frameworks: Synthesis, structures, and hydrogen adsorption properties, Inorg. Chem. 50 (2011) 7555–7562. doi:10.1021/ic2004485.

[5]   Z.H. Xuan, D.S. Zhang, Z. Chang, T.L. Hu, X.H. Bu, Targeted structure modulation of "pillar-layered" metal-organic frameworks for CO2 capture, Inorg. Chem. 53 (2014) 8985–8990. doi:10.1021/ic500905z.

[6]   M. Köberl, M. Cokoja, W.A. Herrmann, F.E. Kühn, From molecules to materials: molecular paddle-wheel synthons of macromolecules, cage compounds and metal-organic frameworks., Dalt. Trans. 40 (2011) 6834–6859. doi:10.1039/c0dt01722a.

[7]   M. Du, C.P. Li, C. Sen Liu, S.M. Fang, Design and construction of coordination polymers with mixed-ligand synthetic strategy, Coord. Chem. Rev. 257 (2013) 1282–1305. doi:10.1016/j.ccr.2012.10.002.

[8]   D. Balestri, A. Bacchi, P. Scilabra, P. Pelagatti, Extension of the Pd-catalyzed CN bond forming reaction to the synthesis of large polydentate ligands containing NH functions, Inorg. Chim. Acta. (2017). doi:10.1016/j.ica.2017.06.029.

[9]   G.. Lausi, A.; Polentarutti, M.; Onesti, S.; Plaisier, J.R.; Busetto, E.; Bais, G.; Barba, L.; Cassetta, A.; Campi, D. Lamba, Status of the crystallography beamline at Elettra, Eur. Phys. J. Plus. (2015) 1–8.

[10] W. Kabsch, Xds, Acta Crystallogr. Sect. D Biol. Crystallogr. 66 (2010) 125–132. doi:10.1107/S0907444909047337.

[11] M.D. Winn, C.C. Ballard, K.D. Cowtan, E.J. Dodson, P. Emsley, P.R. Evans, R.M. Keegan, E.B. Krissinel, A.G.W. Leslie, A. McCoy, S.J. McNicholas, G.N. Murshudov, N.S. Pannu, E.A. Potterton, H.R. Powell, R.J. Read, A. Vagin, K.S. Wilson, Overview of the CCP4 suite and current developments, Acta Crystallogr. Sect. D Biol. Crystallogr. 67 (2011) 235–242. doi:10.1107/S0907444910045749.

[12] P.R. Evans, G.N. Murshudov, How good are my data and what is the resolution?, Acta Crystallogr. Sect. D Biol. Crystallogr. 69 (2013) 1204–1214. doi:10.1107/S0907444913000061.

[13] G.M. Sheldrick, SHELXT - Integrated space-group and crystal-structure determination, Acta Crystallogr. Sect. A Found. Crystallogr. 71 (2015) 3–8. doi:10.1107/S2053273314026370.

[14] O. V. Dolomanov, L.J. Bourhis, R.J. Gildea, J.A.K. Howard, H. Puschmann, OLEX2: A complete structure solution, refinement and analysis program, J. Appl. Crystallogr. 42 (2009) 339–341. doi:10.1107/S0021889808042726.

[15] G.M. Sheldrick, Crystal structure refinement with SHELXL, Acta Crystallogr. Sect. C Struct. Chem. 71 (2015) 3–8. doi:10.1107/S2053229614024218.

[16] L. Ma, L. Wang, Y. Wang, S.R. Batten, J. Wang, Self-Assembly of a Series of Cobalt (II) Coordination Polymers Constructed from H 2 tbip and Dipyridyl-Based Ligands, Inorg. Chem. 48 (2009) 915.

[17] V.A. Blatov, A.P. Shevchenko, D.M. Proserpio, Applied Topological Analysis of Crystal Structures with the Program Package ToposPro, Cryst. Growth Des. 14 (2014) 3576–3586. doi:10.1021/cg500498k.

[18] D.M. Proserpio, V. A. Blatov, L. Carlucci, G. Ciani, Interpenetrating metal–organic and inorganic 3D networks: a computer-aided systematic investigation. Part I. Analysis of the Cambridge structural database, CrystEngComm. 6 (2004) 377–395. doi:10.1039/B409722J.

[19] M.D. Allendorf, M.E. Foster, V. Stavila, P.L. Feng, F.P. Doty, K. Leong, E.Y. Ma, S.R. Johnston, A.A.

Revised

Talin, Guest-Induced Emergent Properties in Metal − Organic Frameworks, (2015). doi:10.1021/jz5026883.

[20]   A.M. Ullman, J.W. Brown, M.E. Foster, K. Leong, V. Stavila, M.D. Allendorf, Transforming MOFs for Energy Applications Using the Guest @ MOF Concept, (2016). doi:10.1021/acs.inorgchem.6b00909.

[21]   J.E. Mondloch, O. Karagiaridi, O.K. Farha, J.T. Hupp, Activation of metal–organic framework materials, CrystEngComm. 15 (2013) 9258. doi:10.1039/c3ce41232f.